Chapter 1

Effect of Processing Conditions on Microstructure: Al–Cu–Si Eutectic Alloy[1]

Uğur Büyük[2]

Abstract

Aluminium is widely used in various industries such as food, electrical and electronics, automotive, aerospace and construction due to its favorable properties such as malleability, corrosion resistance, environmental resistance and high strength-to-weight ratio. In aluminum-based casting alloys, the main alloying elements commonly used in industry are silicon, copper and magnesium. In this study, the microstructure properties of the Al–26.5Cu–6Si (wt.%) ternary eutectic alloy were examined in relation to directional solidification. The alloy was processed in a vacuum melting furnace and solidified directionally at various growth rates using a Bridgman type device. The experimental results revealed eutectic transformation of the Al–26.5Cu6Si alloy, leading to the formation of matrix Al, lamella Al_2Cu, and plate Si phases. Eutectic spacing was measured from the produced samples, and it was found that the values were significantly affected by the growth rate. The results of this study were compared to the experimental results of binary Al–Cu and ternary Al–Cu–Si-Fe eutectic alloys.

1. INTRODUCTION

The microstructures formed during solidification play a crucial role in determining the physical properties and performance of materials. Therefore, understanding the formation and control of these microstructures is a fundamental challenge in the field of materials science [1-2]. While the formation of microstructure in binary alloys has been thoroughly investigated, both from a theoretical [3] and experimental [4-19] perspective,

1 This research was financially supported by the Scientific and Technical Research Council of Turkey (TUBITAK) with project number: 112T588. The author is grateful to the Scientific and Technical Research Council of Turkey for its financial support.

2 Prof. Dr., Erciyes University, Faculty of Education, Department of Science Education, Kayseri, Turkey, buyuk@erciyes.edu.tr, ORCID: 0000-0002-6830-8349

https://doi.org/10.58830/ozgur.pub426.c1845

the comprehension of this same phenomenon in multicomponent alloys, containing three or more components, is still restricted.

Aluminum has many uses in different industries thanks to its excellent formability, resistance to corrosion and environmental effects, and high strength-to-weight ratio. It is used in various fields such as the food industry, electrical and electronics industry, automotive and aerospace industries, and construction applications. The physical properties of multi-component aluminum alloys depend on the specific chemical composition, particularly the alloying elements and their ratios. Silicon, copper, and magnesium are the predominant alloying elements used in aluminum casting alloys, with residual amounts of iron and zinc. AlSi alloys are prevalent in structural uses, while Al–Si–Cu alloys are mainly utilized in powertrain and transmission applications. In recent years, there has been an increase in the use of Al–Cu–Si alloys in various industries due to their favorable characteristics, which include easy formability, low weight, excellent electrical and thermal conductivity, and high resistance to corrosion.

This study examines the measurement of eutectic spacing (λ) of Al–26.5Cu–6Si (wt.%) eutectic alloy solidified at various rates. The relationships between eutectic spacing and solidification rate were investigated using linear regression analysis and the Hall-Petch equation. Furthermore, the results obtained from this study were compared with experimental findings of binary Al–Cu and ternary Al–Cu–Si–Fe eutectic alloys.

2. EXPERIMENTAL PROCEDURES

This research focuses on the Al-26.5wt.%Cu-6wt.%Si alloy, which was prepared by melting 99.99% pure aluminum, 99.98% pure copper, and 99.97% pure silicon in a vacuum. The alloy was then cast into 10 graphite molds and solidified in a Bridgman furnace, with each sample solidifying at different growth rates ($V=8.25$–$164.80\ \mu m/s$) while maintaining a constant temperature gradient ($G=8.50$ K/mm). After smoothing with SiC abrasive paper, each sample was polished on a Struers TegraPol-15 polishing machine and then etched in a solution containing 95 ml of distilled water and 5 ml of hydrofluoric acid (HF) for 10–15 seconds.

To analyze the microstructures of the alloy samples, images of both longitudinal and transverse sections were taken using a Nikon Eclipse model optical microscope (OM) and a LEO model scanning electron microscope (SEM). Energy dispersive X-ray microanalysis (EDAX) was used to determine the composition of the samples. The eutectic spacing of the

samples was measured using the linear intercept method [19], specifically from the transverse sections. Details of the method are shown in Figure 1 [19].

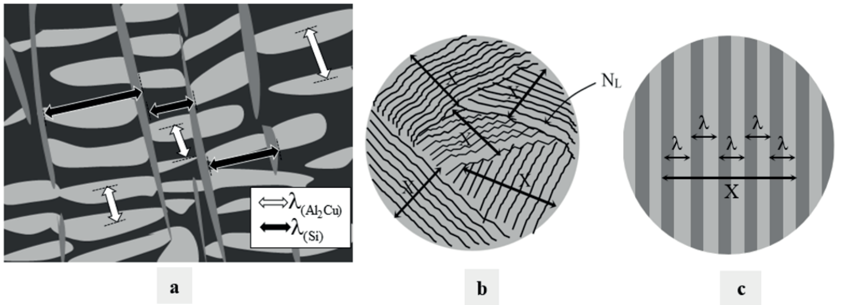

Figure 1. *(a) Measurement of eutectic spacing for directionally solidified Al-Cu-Si eutectic alloy, (b) Schematic view in wide area, (c) Schematic view in narrow area, (linear intercept method:* $\lambda = X/(N_L - 1)$*. Where X, total length of lamella,* N_L *the total number of lamella in the area.*

3. RESULTS AND DISCUSSION

3.1 Effect of growth rate on the eutectic spacing

Figure 2 displays the microstructure of an Al-26.5wt.%Cu-6wt.%Si eutectic alloy, which solidified using a linear growth rate. Several solidification parameters were used to examine the potential phases that could form in Al–Cu–Si alloys. As shown in Figure 2b, when the alloy solidified at a low growth rate and temperature gradient, a wholly developed eutectic microstructure consisting of lamellar and irregular layers within a matrix was observed.

Detailed investigations were conducted on the phase diagram of an Al–based Al–Cu–Si ternary alloy [20] (Figure 3) and the solubilities of the phases that are likely to form within the alloy. It was found that the intermetallic phase Al_2Cu has relatively small solubilities of silicon and copper. Specifically, at the temperature of eutectic transformation (525 ^{o}C), the maximum solubility of copper and silicon in solid aluminum was found to be 4.5Cu and 1.1Si, respectively [21-22]. Moreover, the composition of the samples, consisting of the solid matrix Al, lamellar Al_2Cu, and plate Si phases was quantitatively analyzed using Energy Dispersive X-ray Analysis (EDAX). The obtained results are presented in Table 1. The identification of the different phases presents in the Al-Cu-Si alloy with slow growth

rate, including the α-Al matrix phase, Al_2Cu intermetallic phase, and Si plate phase, was determined using the phase diagram, solubility values, and Energy Dispersive X-ray (EDX) results.

Table 1. *The chemical composition analysis of Al–Cu–Si eutectic alloy by using SEM and EDX.*

Phase	**Al**		**Cu**		**Si**	
	at.%	wt.%	at.%	wt.%	at.%	wt.%
Al_2Cu	80.83	64.17	19.17	35.83		
Al-matrix	97.73	94.81	2.27	5.19		
Si					100	100
Composition	79.19	66.47	13.92	27.52	6.89	6.02

The microstructures of the samples were observed to undergo changes based on the growth rates, with the measurements indicating a decrease in eutectic spacing as the growth rate increases. At a constant temperature gradient, the maximum eutectic spacing was exhibited by the lowest growth rate (V=164.80 μm/s, G=8.50 K/mm), while the minimum eutectic spacing was found for the highest growth rate (V=8.25 μm/s, G=8.50 K/mm). As the growth rate increased from 8.25 to 164.80 μm/s, the average spacing between phases of Al_2Cu decreased from 5.66 μm to 1.35 μm, and the average spacing between phases of Si decreased from 6.42 μm to 1.28 μm.

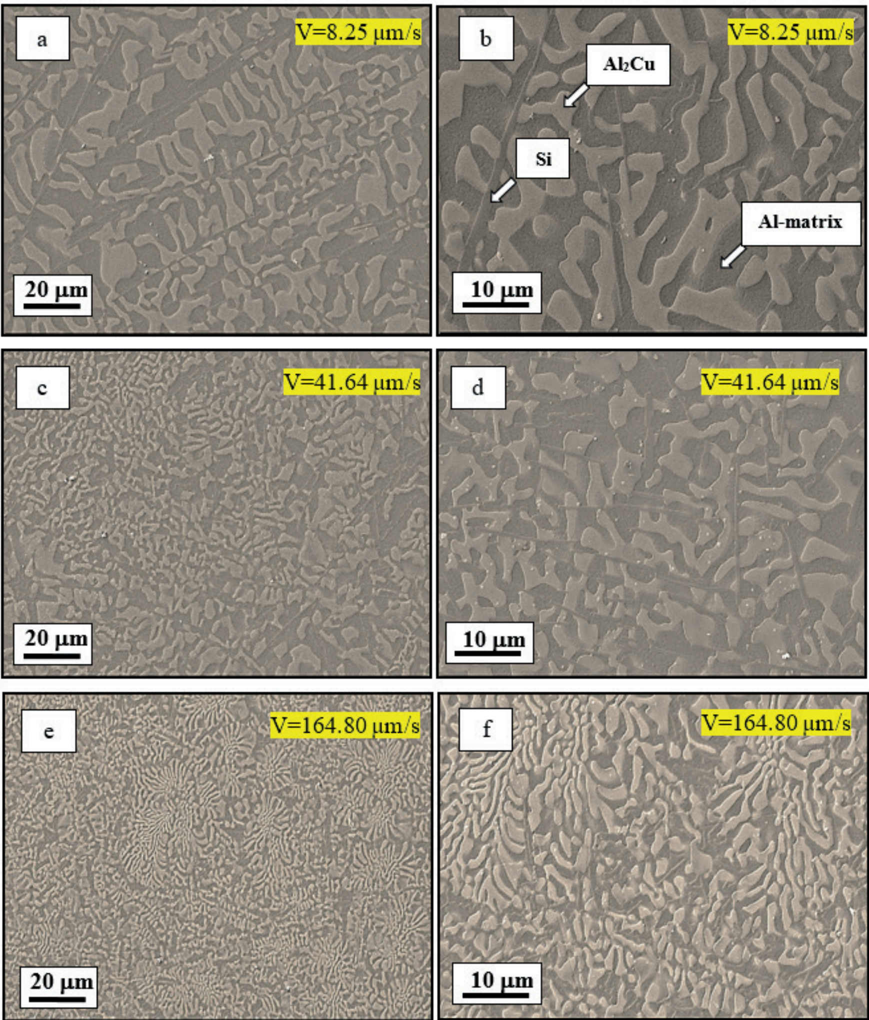

Figure 2. *Typical SEM images of the growth morphologies of directionally solidified Al-Cu-Si eutectic alloy with different growth rate (V=8.25-164.80 µm/s) at a constant temperature gradient (G=8.25 K/mm). (a) – (b) for V=8.25 µm/s, (c) – (d) for V=41.64 µm/s, (e) – (f) for V=164.80 µm/s.*

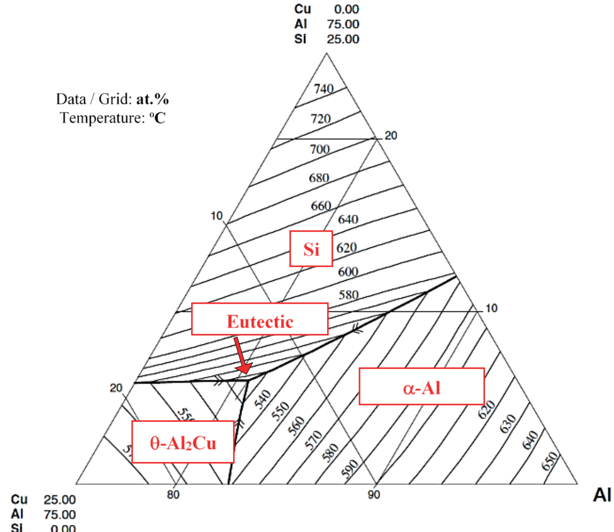

Figure 3. *The liquidus projection of the ternary Al-Si-Cu phase diagram at the Al-rich corner [20].*

Figure 4 presents SEM and optical microscope images of Al–Cu–Si alloys solidified directionally, including Al–Cu–Si [This study], Al–Cu [17], and Al–Cu–Si–Fe [18]. In Figure 4(a), the Al–Cu binary eutectic exhibits regularly arranged Al_2Cu phases in the form of lamellae, while the regularity is somewhat disrupted in the presence of silicon, as shown in Figures 4(b-c). In this study, the Si phases present in the directionally solidified Al-Cu-Si ternary eutectic are observed as irregular plates. Figure 2(e) illustrates that, with an increasing growth rate, Si phases form colonies. According to Hunt and Jackson [3], the high ΔS/R ratio is the primary reason. Here, ΔS denotes the fusion entropy and R represents the gas constant. In Al-Si eutectic alloy, the ΔS/R ratio is high for silicon (3.59), thereby inhibiting the simultaneous growth and formation of regular aligned structures [23].

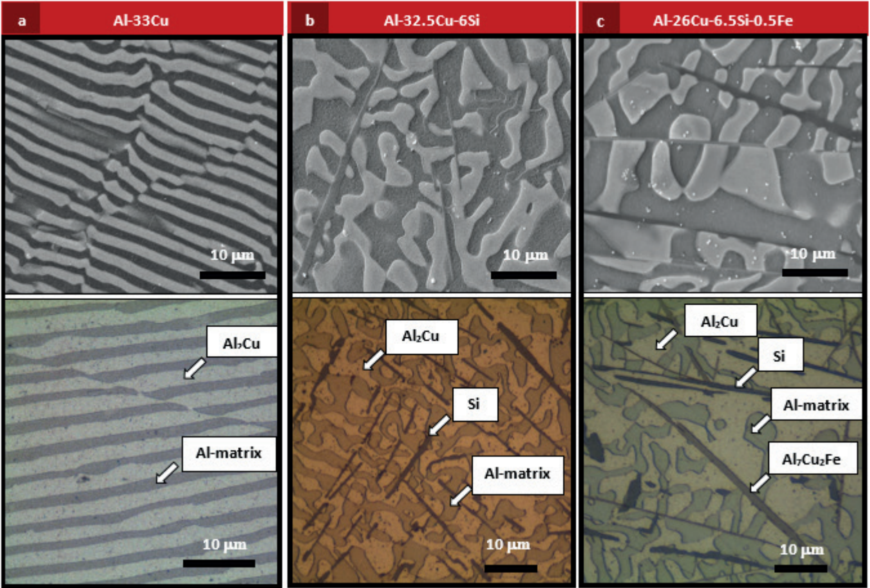

Figure. 4 *Typical SEM (up) and optical (down) images of the growth morphologies of directionally solidified Al-Cu, Al-Cu-Si and Al-Cu-Si-Fe eutectic alloy at a constant growth rate (V=8.25 µm/s) and temperature gradient (G=8.50 K/mm). (a) for Al-Cu eutectic alloy [17], (b) Al-Cu-Si eutectic alloy [This work] and (c) Al-Cu-Si-Fe eutectic Alloy [18].*

During the solidification process of the Al-Cu-Si alloy, the interface between the Al_2Cu and Si phases has lost its planarity, resulting in the formation of phases that rise towards the liquid phase, as illustrated in Figure 5(a). At high solidification rates, as depicted in Figure 5(b), regular local lamella structures have been observed in certain regions. Table 2 displays the changes in average eutectic intervals based on growth rate. Accordingly, since the microstructure changes in a logarithmic pattern with the growth rate, we utilized linear regression analysis to establish theoretical and statistical relationships between the variable parameters.

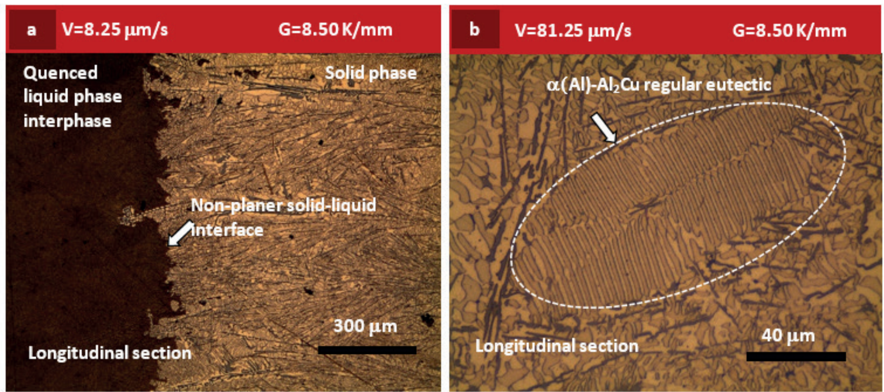

***Figure 5** a) The solid–liquid non-planar interface, during unidirectional solidification process, b) The local regular eutectic zone at high growth rates. (V=81.25 µm/s) for Al–Cu–Si eutectic alloy.*

***Table 2.** The values of microstructure, microhardness, ultimate tensile–strength and electrical resistivity for directionally solidified ternary Al–Cu–Si eutectic alloy.*

Alloys (wt%.)	Solidification Parameters		Eutectic Spacing	
	G (K/mm)	V (µm/s)	$\lambda_{(Al_2Cu)}$ (µm)	$\lambda_{(Si)}$ (µm)
		8.25	5.66	6.42
		16.60	4.25	4.70
Al-26.5Cu-6Si	8.50	41.65	2.83	2.69
		90.05	2.01	1.91
		164.80	1.35	1.28

The relationship between eutectic spacing and growth rate is given in Figure. 6. The correlation between variables was determined as $\lambda_{(Al_2Cu)} = 15.39\ V^{-0.53}$ and $\lambda_{(Si)} = 20.49\ V^{-0.54}$. The results were compared with Al–Cu eutectic alloy and presented in Table 3. Experimentally obtained exponential value are the most important parameters that give the relationship between the growth rate and microstructure of alloys. In this study, 0.53 and 0.54 exponential value were calculated for Al_2Cu eutectic lamellae and Si eutectic plates, respectively, in Al–Cu–Si ternary eutectic alloy.

When compared to similar studies in the literature, the exponential values obtained for Al_2Cu eutectic spacing in Al-Cu binary alloys were 0.54 [17] and 0.40 [15], while the values obtained for Al_2Cu eutectic spacing in Al–Cu–Ag ternary alloys were 0.50 [14], and for Si eutectic plates in Al–Si–Mg ternary alloy, the value was 0.45. The exponential values of Si eutectic plates in Al–Si–Ni ternary alloy, Si eutectic plates in Al–Si binary alloy, and Al_2Cu eutectic lamellae and Si eutectic plates in Al–CuSi–Fe quaternary eutectic alloy were 0.50 [24], 0.46 [12], and 0.50 and 0.55 [18], respectively. Notably, the values derived from this study closely resemble the exponential value of 0.50 projected by Jackson–Hunt eutectic theory [3].

Table 3*. The relationship between the eutectic spacing, microhardness, ultimate tensile strength, electrical resistivity and growth rate for some directionally solidified alloys.*

Alloys (wt%.)	**Microstructure**	**Ref.**
Al–33Cu	$\lambda = 13.52(V)^{-0.54}$	[15]
Al–26.5Cu–6Si	$\lambda_{(Al_2Cu)} = 15.39(V)^{-0.53}$ $\lambda_{(Si)} = 20.49(V)^{-0.54}$	[This work]
Al–26Cu–6.5Si–0.5Fe	$\lambda_{(Al_2Cu)} = 14.74(V)^{-0.50}$ $\lambda_{(Si)} = 25.13(V)^{-0.55}$	[18]

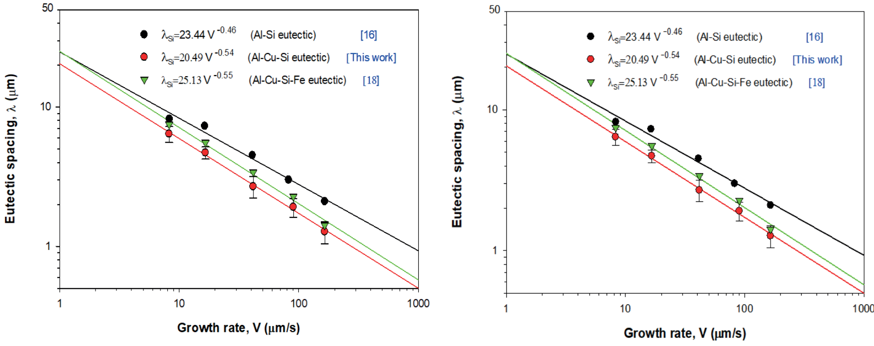

Figure 6. *Variation of eutectic spacing (a) $\lambda_{(Al_2Cu)}$ and (b) $\lambda_{(Si)}$ as a function of growth rate at a constant temperature gradient (G=8.50K/mm) for ternary Al-Cu-Si eutectic alloys and compare with the binary Al-Cu eutectic, Al-Si eutectic and quaternary Al-Cu-Si-Fe eutectic alloys.*

4. CONCLUSION

The results can be summarized as follows: The experimental results revealed eutectic transformation of the Al–26.5Cu–6Si alloy, leading to the formation of matrix Al, lamella Al_2Cu, and plate Si phases. As the growth rate increases from 8.25 to 164.80 µm/s, the eutectic spacing decreases from 5.66 to 1.35 for $\lambda_{(Al_2Cu)}$ and from 6.42 to 1.28 for $\lambda_{(Si)}$. Microstructure were obtained as a function of growth rate: $\lambda_{(Al_2Cu)} = 15.39\ V^{-0.53}$ and $\lambda_{(Si)} = 20.49\ V^{-0.54}$.

ACKNOWLEDGMENTS

This research was financially supported by the Scientific and Technical Research Council of Turkey (TUBITAK) with project number: 112T588. The author is grateful to the Scientific and Technical Research Council of Turkey for its financial support.

REFERENCES

1. De Wilde, J., Nagels, E., Lemoisson, F., & Froyen, L. (2005). Unconstrained growth along a ternary eutectic solidification path in Al–Cu–Ag: Preparation of a MAXUS sounding rocket experiment. *Materials Science and Engineering: A*, *413*, 514-520.
2. Morando, C., & Fornaro, O. (2018). Morphology and phase formation during the solidification of Al-Cu-Si and Al-Ag-Cu ternary eutectic systems. *Materials Research*, *21*.
3. Jackson KA, Hunt JD. 1966. Lamellar and Rod Eutectic Growth. *Transactions of Metallurgic Society of AIME* 226, 1129-1142.
4. McCartney, D. G., Hunt, J. D., & Jordan, R. M. (1980). The structures expected in a simple ternary eutectic system: Part 1. Theory. *Metallurgical Transactions A*, *11*, 1243-1249.
5. McCartney, D. G., Jordan, R. M., & Hunt, J. D. (1980). The structures expected in a simple ternary eutectic system: Part II. The Al-Ag-Cu ternary system. *Metallurgical Transactions A*, *11*, 1251-1257.
6. Himemiya, T., & Umeda, T. (1999). Three-phase planar eutectic growth models for a ternary eutectic system. *Materials Transactions, JIM*, *40*(7), 665-674.
7. Himemiya, T. (1999). Growth models of two-phase eutectic cell in a ternary eutectic system: a phase selection map. *Materials transactions, JIM*, *40*(7), 675-684.
8. Himemiya, T. (2000). Extension of cellular/dendritic eutectic growth model to off-monovariant range: Phase selection map of a ternary eutectic alloy. *Materials transactions, JIM*, *41*(3), 437-443.
9. Hecht, U., Gránásy, L., Pusztai, T., Böttger, B., Apel, M., Witusiewicz, V., ... & Rex, S. (2004). Multiphase solidification in multicomponent alloys. *Materials Science and Engineering: R: Reports*, *46*(1-2), 1-49.
10. Böyük, U., & Maraşlı, N. (2009). The microstructure parameters and microhardness of directionally solidified Sn–Ag–Cu eutectic alloy. *Journal of alloys and compounds*, *485*(1-2), 264-269.
11. Çadırlı, E., Böyük, U., Kaya, H. A. S. A. N., Maraşlı, N., Keşlioğlu, K., Akbulut, S., & Ocak, Y. (2009). The effect of growth rate on microstructure and microindentation hardness in the In–Bi–Sn ternary alloy at low melting point. *Journal of Alloys and Compounds*, *470*(1-2), 150-156.
12. Böyük, U., Engin, S., & Maraşlı, N. (2011). Microstructural characterization of unidirectional solidified eutectic Al–Si–Ni alloy. *Materials Characterization*, *62*(9), 844-851.

13. Böyük, U., Engin, S., Kaya, H. A. S. A. N., & Maraşlı, N. (2010). Effect of solidification parameters on the microstructure of Sn-3.7 Ag-0.9 Zn solder. *Materials characterization*, *61*(11), 1260-1267.
14. Böyük, U., Maraşlı, N., Kaya, H. A. S. A. N., Çadırlı, E., & Keşlioğlu, K. (2009). Directional solidification of Al–Cu–Ag alloy. *Applied Physics A*, *95*, 923-932.
15. Cadirli, E., Ülgen, A., & Gündüz, M. (1999). Directional solidification of the aluminium-copper eutectic alloy. *Materials Transactions, JIM*, *40*(9), 989-996.
16. Gündüz, M., Kaya, H., Çadırlı, E., & Özmen, A. (2004). Interflake spacings and undercoolings in Al–Si irregular eutectic alloy. *Materials Science and Engineering: A*, *369*(1-2), 215-229.
17. Engın, S., & Büyük, U. (2018). Variations with Growth Rate of The Microstructurel, Mechanical and Electrical Properties of Directionally Solidified The Al-Cu Alloy. *GÜFBED/GUSTIJ*, *8*, 2-209.
18. Büyük, U., Engin, S., Kaya, H., Çadırlı, E., & Maraşlı, N. (2020). Directionally Solidified Al–Cu–Si–Fe Quaternary Eutectic Alloys. *Physics of Metals and Metallography*, *121*(1), 78-83.
19. Ourdjini, A., Liu, J., & Elliott, R. (1994). Eutectic spacing selection in Al–Cu system. *Materials Science and Technology*, *10*(4), 312-318.
20. Lukas H.L., Lebrun N., Al–Cu–Si (Aluminium–Copper–Silicon) G. Effenberg, S. Ilyenko (Eds.), SpringerMaterials - The Landolt-Börnstein Database, pp. 135-147, 2005.
21. Zolotorevsky V.S., Belov N.A., Glazoff M.V. Casting aluminium alloys. 1st ed. pp. 83-85, Elsevier, 2007.
22. Mondolfo L.F., Metallography of aluminum alloys, John Wıley & Sons, Inc. New York, pp. 86-87, 1943.
23. Rohatgi, P. K., Sharma, R. C., & Prabhakar, K. V. (1975). Microstructure and mechanical properties of unidirectionally solidified Al-Si-Ni ternary eutectic. *Metallurgical Transactions A*, *6*, 569-575.
24. Kaygısız, Y., & Maraşlı, N. (2015). Microstructural, mechanical and electrical characterization of directionally solidified Al–Si–Mg eutectic alloy. *Journal of Alloys and Compounds*, *618*, 197-203.